2017

Using Lower Extremity Muscle Activations to Estimate Human Ankle Impedance in the External-Internal Direction

Lauren N. Knop
Michigan Technological University, lknop@mtu.edu

USING LOWER EXTREMITY MUSCLE ACTIVATIONS TO ESTIMATE HUMAN ANKLE IMPEDANCE IN THE EXTERNAL-INTERNAL DIRECTION

By

Lauren N. Knop

A REPORT

Submitted in partial fulfillment of the requirements for the degree of

MASTER OF SCIENCE

In Mechanical Engineering

MICHIGAN TECHNOLOGICAL UNIVERSITY

2017

This report has been approved in partial fulfillment of the requirements for the Degree of MASTER OF SCIENCE in Mechanical Engineering.

Department of Mechanical Engineering – Engineering Mechanics

Report Advisor:	*Mo Rastgaar*
Committee Member:	*Nina Mahmoudian*
Committee Member:	*Ye Sun*
Committee Member:	*Timothy Havens*
Department Chair:	*William W. Predebon*

Table of Contents

Acknowledgements

I would like to thank my advisor, Dr. Mo Rastgaar, for providing me with this opportunity and keeping me on the right track.

I am grateful for the members of the Human Interactive Robotics Lab, including Dr. Houman Dallali, Dr. Evandro Ficanha, Leslie Castelino, and Guilherme Ribeiro, as they have helped with experimental work, answered many questions, and provided much guidance as I continue my career. I thank you for your time and effort.

Last, I would like to thank the National Science Foundation for supporting this work under CAREER Grant No. 1350154.

Abstract

For millions of people, mobility has been afflicted by lower limb amputation. Lower extremity prostheses have been used to improve the mobility of an amputee; however, they often require additional compensation from other joints and do not allow for natural maneuverability. To improve upon the functionality of ankle-foot prostheses, it is necessary to understand the role of different muscle activations in the modulation of mechanical impedance of a healthy human ankle. This report presents the results of using artificial neural networks (ANN) to determine the functional relationship between lower extremity electromyography (EMG) signals and ankle impedance in the transverse plane. The Anklebot was used to apply pseudo-random perturbations to the human ankle in the transverse plane, while motion of the ankle in the sagittal and frontal planes was constrained. Using a stochastic system identification method, the mechanical impedance of the ankle in external-internal (EI) direction was determined as a function of the applied torque and corresponding ankle motion. The impedance of the ankle and muscle EMG signals were determined for three muscle activation levels, including with relaxed muscles, and with muscles activated and 10% and 20% of the subject's maximum voluntary contraction (MVC). This information was used as the input and target matrices to train an ANN for each subject. The resulting ankle impedance from the proposed ANN was effectively predicted within 85% accuracy for nine out of ten subjects, and was within ±5 Nm/rad of the target impedance for all subjects. This work provides more understanding of the neuromuscular characteristics of the ankle and provides insight toward future design and control of ankle-foot prostheses.

1 Introduction

In the United States alone, more than 2 million people have suffered the loss of a limb, majority of which are trans-tibial amputations of the lower extremity [1, 2]. Despite efforts to decrease the number of amputations, the number of amputees have been increasing at a rate of at least 185,000 people each year since 2005 and is expected to affect approximately 3.6 million people by the year 2050. Typical trans-tibial amputees will use an ankle-foot prosthesis to regain maneuverability. However, most existing ankle-foot prosthesis develop challenges for amputees, as they do not allow for a natural gait cycle [3, 4]. To improve upon this issue, it is necessary to understand the function of a healthy human ankle to better improve the design and control of ankle-foot prostheses.

The ankle is the first major joint to be in contact with the ground during locomotion, and must be able to transfer ground reaction forces to the body. This is important for maintaining balance during standing, shock absorption during walking, and ambulation during other activities of daily living (ADL), such as climbing stairs, turning a corner, maneuvering an obstacle, or walking on uneven ground. By changing the lower extremity muscles contraction levels, the mechanical impedance of the ankle changes to provide the appropriate shock absorption or propulsion during a movement. The impedance can be defined as the resulting torque caused by an external perturbation to the foot, and can vary based on the effects of mass-inertia, damping, and stiffness [5].

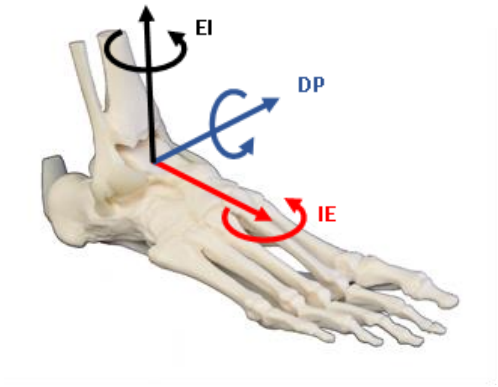

Figure 1. Axes of ankle rotation in the sagittal (DP), frontal (IE), and transverse (EI) anatomical planes.

During ADL, the impedance of the ankle can be modulated about the dorsiflexion-plantarflexion (DP), internal-external (IE), and external-internal (EI) degrees of freedom (DOF), as shown in Fig. 1. These motions correspond to ankle modulation in the sagittal, frontal, and transverse anatomical planes, respectively. Although many gait studies have

only focused on the ankle during DP rotation, the ankle is also highly dependent on function in IE and EI, especially during turning maneuvers [6, 7]. In fact, it has been shown that turning steps make up approximately 8-50% of the total steps completed in a single day [8]. Understanding the properties of the ankle in all three DOF will provide insight to develop effective assistive and rehabilitation devices.

Initial studies of the ankle worked to model the ankle properties in the sagittal plane (DP). A linear second order model of the ankle's inertia, damping, and stiffness properties was determined by varying the mean ankle torques and the displacement amplitude applied to the foot [9, 10]. These studies determined that, while the inertial effects remained constant, the stiffness and damping parameters increased as the mean torque increased, and decreased as the ankle displacement amplitude increased. In addition, a continuation of these studies also determined that the stiffness and damping properties of the ankle are dependent upon ankle position and muscle activation level [11, 12]. Similar work estimated the active stiffness properties of the ankle in the IE direction by applying perturbations to the ankle with the use of a swaying cradle [13]

Furthermore, a series of studies developed a multivariable stochastic system identification method to estimate the quasi-static and dynamic impedance of the ankle in the sagittal, frontal, and transverse planes under stationary conditions [14-21]. The Anklebot, a back drivable and safe rehabilitation robot, consists of two linear actuators that apply pseudo-random perturbations to the ankle, and measures the resulting angle and torque response. The Anklebot actuators were placed parallel to the shank and applied pseudo-random perturbations to the foot in both dorsi-plantarflexion and internal-external motions to determine the impedance in the DP and IE directions. This coupled, multivariable impedance was determined for both relaxed and active muscle co-contraction and a dynamic model for each condition was proposed in [22]. In addition, the same stochastic system identification method was applied to determine the impedance of the ankle in the EI direction [17]. The only difference was that the actuators were placed parallel to the ground, and perturbed the foot in the transverse plane.

These studies quantified ankle impedance while the subjects were seated and held static muscle contraction levels; however, ankle impedance changes during ADL. The Anklebot was employed to determine the time-varying impedance of the ankle of the ankle in the DP and IE directions during the swing phase of gait, while walking on a treadmill [23]. Additionally, the time-varying impedance of the ankle during the stance phase was determined during walking with the use of perturbation and force plate walking platforms [24-26]. It was concluded that the ankle impedance in the DP and IE directions varied greatly throughout the gait cycle. The impedance parameters determined from these studies has led to developments in powered ankle-foot prostheses that are controllable in both the DP, IE, and EI directions [27-30].

Advancements in ankle-foot prostheses has also led to advancements in methods for controlling the prostheses and allowed for improved use based on the amputee's intentions. One promising method to improve control uses electromyography (EMG) to measure the electrical activity of a muscle as it contracts at different magnitudes [31]. Using this information, the relationship between muscle activation level and joint dynamics can be determined [32]. Previous work has determined the stiffness and torques of the elbow and shoulder joints based on upper extremity EMG signals [33, 34]. In addition, lower extremity EMG signals have been used in proportional control of a powered ankle-foot orthosis and robotic ankle exoskeleton [35, 36]. Few groups have applied the use of artificial neural networks (ANN) to determine the linear or nonlinear relationship between muscle activation and both upper and lower extremity joint stiffness, angles, and torques [37-40].

Recently, in an effort to find a practical relationship between the muscle signals to complex impedance properties of the ankle, a method was developed to determine the relationship between lower extremity muscle activation levels and ankle impedance in the DP and IE directions with an ANN [41]. Using the stochastic impedance estimation method that was previously described, the Anklebot determined the ankle impedance of nine subjects in the DP and IE directions. The experiment was repeated to determine the impedance for three different levels of muscle activations and the resulting impedance was used as the target for training the ANN. The root-mean-squared (rms) of the tibialis anterior (TA), peroneus longus (PL), soleus (SOL) and gastrocnemius (GA) muscles of the lower leg, selected based on their contribution to ankle motion, were used for training the ANN [42]. The resulting ANN models could estimate the ankle impedance based on EMG signals with approximately 89% mean accuracy in DP and 88% mean accuracy in IE.

The goal of this study was to fill the remaining gap in understanding the relationship between muscle activation levels and the mechanical impedance of the ankle in the transverse plane (EI). As a continuation of the efforts in the sagittal (DP) and frontal planes (IE), this study proposed to use a similar approach to use the lower extremity muscle EMG to define the ankle dynamic impedance in the transverse plane. This study determined the ankle impedance of ten subjects, five male and five female, with relaxed muscles, and with 10% and 20% of the maximum voluntary contraction (MVC) of the muscles. An improved method used ANN to define the functional relationship between the impedance and muscle activity. The results from this study contribute to understanding the ankle dynamics in the transverse plane from a musculoskeletal point of view. In addition, this work can be used as a proof of concept for future control design for ankle-foot prosthesis.

2 Methods

2.1 Experimental Setup

Ten subjects (five male, five female with ages from 22 to 33 and average BMI of 23.8 ± 4.3 kg/m2) with no self-reported neuromuscular or biomechanical disorders participated in this study. This research was approved by the Michigan Technological University Institutional Review Board, and each subject gave written consent to participate in the experiment.

Previous work has used the Anklebot to estimate the ankle impedance in the DP, IE, and EI directions [17, 19]. This experiment replicated the procedure to determine the ankle impedance in the transverse plane [18] . The Anklebot is composed of two back-drivable linear actuators that apply torque and position perturbations in the transverse plane of the ankle. The applied torque and angular displacement of the ankle were recorded at 200 Hz using current sensors (Burr-Brown 1NA117P), with a nominal resolution of $2.56x10^{-6}$ Nm, and two linear incremental encoders (Reinshaw®), with a resolution of $5x10^{-6}$m. Based on previous testing protocols, the Anklebot was controlled in active impedance mode with an active angular stiffness of 12.8 Nm/rad and zero damping in order to prevent drift and hold the foot near the center position [18]. Pseudo-random voltage inputs with a bandwidth of 100 Hz were applied in equal magnitude and opposite direction to each actuator. These perturbations resulted in a maximum torque of 15 Nm and a rms rotation of 0.065 rad about the ankle.

As shown in Fig. 2, the subjects were seated in a custom-made chair and a shoe, with an aluminum bracket (2) attached to the sole, was placed on the right foot. The Anklebot (1) was mounted underneath the seat of the chair and the moving ends of each linear actuator were attached to the shoe bracket. As the actuators moved, a torque perturbation caused the ankle to rotate in the EI direction. To ensure that the foot was only rotated in the transverse plane, the adjustable bar (3) was positioned so that the actuators of the Anklebot were parallel to the ground. A knee brace (4) and supporting straps (5) were used to support the weight of the subject's leg and maintain the horizontal position of the Anklebot. Last, a shin brace (6) was used to prevent any motion of the leg in the sagittal plane caused by the forces applied from the actuators.

The muscles selected to be monitored throughout the test were chosen based on their contribution to ankle motion in the transverse plane, as well as the sagittal and frontal planes. Ankle motion in all three DOFs occurs through a combination of rotations about the talocrural joint and the subtalar joint, otherwise known as the talocrural/subtalar complex [42-44]. The muscles chosen for this experiment directly correlate to the motion of the talocrural/subtalar complex and include the TA (7), PL (8), SOL (9), and GA (10) muscles. Muscle activity was measured using the Delsys® Trigno™ Wireless surface EMG sensors and the raw signals were sampled at 1925 Hz, low-pass filtered at 500 Hz, and a motion artifact suppression was applied to reduce low frequency noise. Rubbing alcohol was used to clean the subjects' skin, and then each sensor was placed at the center of the desired muscle with the use of hypoallergenic tape.

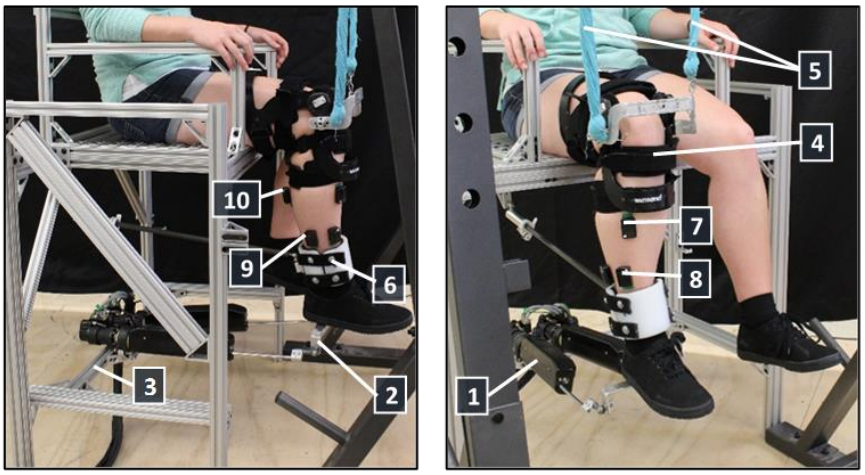

Figure 2. Experimental Setup of the Anklebot to measure ankle impedance in the transverse plane and EMG sensor placement to measure muscle activation levels.

2.2 Experimental Protocol

The experimental protocol consisted of one test to determine the maximum voluntary contraction (MVC) of the muscles of interest, and three tests to correlate the ankle impedance with different levels of muscle co-contraction. First, each subject co-contracted their muscles of interest to the maximum level possible, while keeping a neutral ankle angle. The highest EMG voltage of the TA muscle was recorded and used as the reference MVC level throughout the experiment.

Next, Fig. 3 shows that the Anklebot applied perturbations to the ankle in the EI direction for 70 seconds and the resulting ankle angles and torques were recorded. These measurements were used in a stochastic identification system to determine the ankle impedance, as described later in *Target Matrix* section. For the duration of the experiment the surface EMG signals of the lower leg muscles were recorded as the subject held their muscle activations at a relaxed level, at 10% of their MVC, and at 20% of their MVC. These levels of activation were selected because they were easily sustainable for the subject during the 70 second duration. To ensure repeatability, the test at each muscle activation level was repeated five times, for a total of 15 tests. The subjects watched the EMG signal of their TA muscle on a computer screen and adjusted their co-contraction levels to remain constant for the entire trial. After 15 tests were completed, the data was saved and truncated to 60 seconds to remove transient data at the start of each trial.

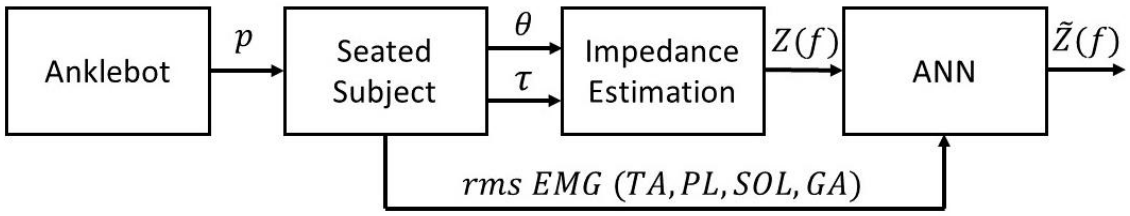

Figure 3. Block diagram of the experimental process used to determine ankle impedance, muscle EMG, and to train the ANN, where p is the perturbation caused by Anklebot, θ and τ are the measured ankle angles and torques, $Z(f)$ is the experimental impedance determined from a stochastic identification method, and $\tilde{Z}(f)$ is the ANN estimated impedance.

2.3 Artificial Neural Networks

2.3.1 ANN Overview

The goal of this study was to develop a model to define the relationship between different levels of lower leg muscle activations and the frequency dependent mechanical impedance of the ankle. This functional relationship can be defined as:

$$\boldsymbol{y} = g(\boldsymbol{x}, f) \tag{1}$$

where $\boldsymbol{y}$ is the impedance of the ankle determined by the rms values of four EMG signals, $\boldsymbol{x}$, and the impedance frequency range, f. Machine learning is one technique that can use function approximation to define the complex relationship between data, without requiring an already existing model of the system. The ANN method selected for this study was a multi-layered network with regression because of its ability to estimate both linear and nonlinear function approximations.

The Matlab® Neural Network Toolbox was used during this study to develop a multilayered feedforward neural network for function approximation. As shown in Fig. 4, each network consists of five input neurons, a hidden layer with sixty neurons, and an output layer with two neurons. Each neuron is connected by a series of weights and biases throughout the network. The neurons of the hidden and output layers are equal to the product of the net input and the weight, ω_{ij} or ε_{jk}, plus a constant bias, $b_{1\ldots60}$. As the network is trained, the weights and biases are tuned to reach the optimal network performance [45]. Sixty hidden layer neurons were selected based the results of an initial test that trained the ANN with a hidden layer ranging between 10 – 200 neurons. The relative error between the experimental and ANN estimated impedance was smallest around 60 neurons, suggesting that networks with fewer neurons could not sufficiently fit the data and networks with greater neurons overfit the data.

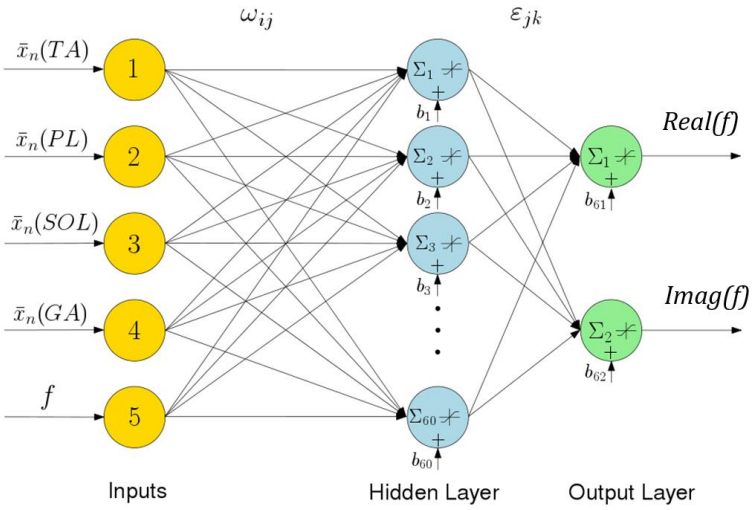

Figure 4. The feedforward network, including 5 input nodes, 60 hidden layer neurons, and 2 output layer neurons. The weights are ω_{ij} and ε_{jk}, where i=1,…,5 , j=1,…,50, and k=1,2, and constant biases are shown from $\{b_1, b_2, \dots, b_{60}\}$ in the hidden and output layers.

2.3.2 Input Matrix

The input matrix consisted of five nodes. Four of these nodes contained the rms of each EMG signal inputs, generated by the TA, PL, SOL, and GA muscles, and one input for the desired impedance frequency range. First, the overall rms of the EMG signal for the relaxed, 10% MVC, and 20% MVC trials were determined. The signal of the relaxed EMG had a small offset, resulting in a magnitude that ranged between 0 to ±20 μv for the four muscles. To remove this offset, each round of experiments was normalized with respect to the relaxed muscle test, as shown in Eq. 2, where $\bar{x}$ is the rms EMG signal, and n is the trial from 1 to 15.

$$\overline{x_n} = \frac{\bar{x}}{passive\ \bar{x}} \tag{2}$$

The input matrix also included an input node for the desired impedance frequency range of 0.7 – 4.1 Hz, selected because it is less than the break frequency where inertial effects dominate the impedance frequency response. Within this frequency range, the impedance magnitude is dominated by the visco-elastic properties of the ankle (stiffness and damping) and remains nearly constant [18]. This range was fixed for all trials, resulting in a total of 18 frequency points to define the impedance. The input submatrix for a single test took the form:

$$(r_n)_{5x18} = [\ \bar{x}_n(TA)\ \ \bar{x}_n(PL)\ \ \bar{x}_n(SOL)\ \ \bar{x}_n(GA)\ \ \ f\ \ ]^T \tag{3}$$

where r_n is the matrix for a single test with an index $n = \{1, \dots, 15\}$, for the 15 total tests performed. The overall input matrix, R, used for the ANN model is composed of all 15 submatrices from Eq. 3. As shown in Eq. 4, the overall matrix contains the r_1 matrix,

which corresponds to the first relaxed muscle test, the r_2 is the first 10% MVC test, the $r_3$is for the first 20% MVC test, with a repeating pattern up to r_{15}.

$$R = [\ r_1\ \ r_2\ \ r_3\ \ \dots\ \ r_{15}\ ]_{5x270} \tag{4}$$

2.3.3 Target Matrix

The target matrix was used to train each ANN model and was composed of the ankle impedance in the frequency domain, estimated from a stochastic identification method. This type of method was selected because of its ability to provide a quantitative estimate of the impedance, without requiring any *a priori* knowledge about its order or dynamic structure [46]. The ankle impedance was estimated for the three levels of muscle activations, including relaxed, 10% MVC, and 20% MVC. During each trial, the Anklebot actuators applied a torque to the ankle and measured the resulting ankle angle in the transverse plane. Assuming linear dynamics, the mechanical impedance of the ankle can be described as a linear, time-invariant transfer function relating input ankle motion to output torques.

The total impedance of the system was estimated using the *tfestimate* function in Matlab®. This function implements Welch's averaged-modified periodogram method to find the transfer function, based on the quotient of the cross power spectral density of the angular displacement and total torque applied to the system, $P_{\tau\theta}$, and the auto power spectral density of the input angles, $P_{\theta\theta}$ (Eq. 5). Based on previous work, the *tfestimate* parameters were selected to use a Hamming window with a length of 512 samples and 50% overlap (256 samples), a sampling frequency of 200 Hz, and a FFT length of 1024 samples, yielding a spectral resolution of 0.195 Hz.

$$Z(f) = \frac{P_{\tau\theta}(f)}{P_{\theta\theta}(f)} \tag{5}$$

In addition, the magnitude-squared coherence of the transfer function is defined in Eq. 6, where $P_{\tau\tau}(f)$ is the auto-power spectral density of the output torque. The *mscohere* function in Matlab® was used to validate the linearity assumption during the impedance estimation across the 0.7 - 4.1 Hz frequency range.

$$C_{\tau\theta} = \frac{|P_{\tau\theta}(f)|^2}{P_{\tau\tau}(f)P_{\theta\theta}(f)} \tag{6}$$

During each test, the Anklebot measured the overall torques and angles generated from both the subject's ankle and the Anklebot system. The angle produced is shared by the Anklebot actuators, shoe, and ankle; therefore, the impedance of the ankle and Anklebot are in parallel. To determine the impedance of the ankle alone, the impedance of the Anklebot, without a human subject, was subtracted from the total system impedance (Eq. 7). Using the same procedure, an additional test was performed without a human subject to determine the impedance of the Anklebot.

$$Z_{ankle} = Z_{ankle+Anklebot+shoe} - Z_{Anklebot+shoe} \tag{7}$$

The resulting ankle impedance were presented in complex form, and the real and imaginary coefficients were used to build the target output submatrix. The submatrix for a single trial took the form shown in Eq. 8,

$$y_i = \begin{bmatrix} Real_i(f) \\ Imag_i(f) \end{bmatrix}_{2x18} \tag{8}$$

where $i = \{1, 2, 3, \dots, 15\}$. Once the impedance was determined for all 15 trials, the submatrices were combined to form a single target matrix with a size of 2x270, as shown in Eq. 9. This matrix was used to train each ANN model, as described in the next section.

$$Y = [\, y_1 \;\; y_2 \;\; y_3 \;\; \dots \;\; y_{15} \,]_{2x270} \tag{9}$$

2.3.4 ANN Training & Validation

The input and target matrices were used to train and validate the ANN models through supervised training. The total data set was randomly divided into three smaller subsets for training, validation, and testing of the model performance. First, 70% of the total data set was used to train the ANN model. The Levenberg-Marquardt backpropagation algorithm was selected to update the weights and biases until the optimal network performance was achieved. To check that the model did not overfit the data, 15% of the total data set was selected for validation and was used to determine how the trained model responded to new input data. When the validation error reached a minimum, the remaining 15% of the total data, not used during training or validation, was used to test the performance of the ANN model. The model for each subject was trained between three and five times until the best fit was achieved.

3 Results & Discussion

3.1 Stochastic System Identification of Ankle Impedance

The resulting ankle impedance estimation, determined from the previously proposed stochastic identification method, can be found in Figs. 5, 6, and 7. Figure 5 shows the magnitude, phase, and coherence of a representative subject for the relaxed, 10% MVC, and 20% MVC. The mean and standard errors for the magnitude and phase were determined at each frequency point across five trials. The standard error was determined using the equation $SE = s/\sqrt{n}$, where s is the standard deviation at each frequency point across five trials and n = 5 for the five repetitions for each test. The mean impedance magnitudes increased as the muscle activation level increased and were similar to results found in previous work [17, 21, 41]. In addition, the average phase and standard errors for the representative subjects for all three tests were less than 90 degrees, verifying that the selected frequency range resulted in an impedance less than the break frequency. Last, the averaged coherence for all ten subjects was greater than 0.88. The high coherence validates the linearity assumption of the impedance identification method within the selected frequency range.

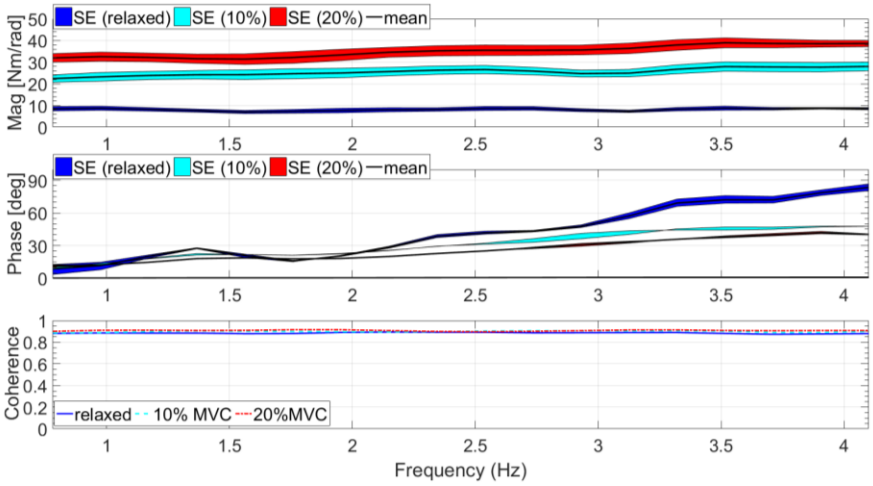

Figure 5. Average magnitude, phase, and coherence of the ankle impedance in the EI direction for a representative subject with relaxed muscles, 10% MVC, and 20% MVC. The shaded areas show the standard errors (SE) at each frequency.

Figures 6 shows the bar plots of the average magnitude and phase across the entire frequency range for all subjects. The whiskers on each bar show the average standard error across the frequency range. As described earlier, the impedance magnitude increased with muscle activation levels and average phase remained less than the 90 degrees phase crossing for all subjects.

The impedance determined through the stochastic system identification method can be compared with the results of previous studies on the ankle impedance in the transverse plane [17, 18]. These studies have determined the mechanical impedance of the ankle with

relaxed muscles and with muscle activations at 10% MVC. The average impedance magnitude found in Figs. 6 and 7 agree with the impedance reported in previous studies, with an average relaxed magnitude of 5.0 ± 1.9 Nm/rad and average 10% MVC magnitude of 15.1 ± 4.6 Nm/rad for the 0.7 – 4.1 Hz frequency range. Furthermore, the impedance magnitude for the 20% MVC has not been reported in the literature and resulted in an average of 19.7 ± 6.3 Nm/rad across ten subjects. The impedance estimations, determined for all ten subjects, were used as the target impedance for training the ANN models.

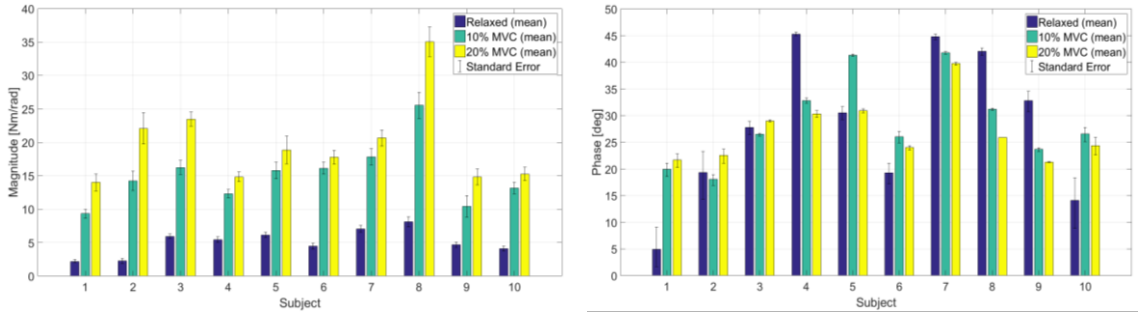

Figure 6. Average impedance magnitude and phase for all the subjects with relaxed, 10% MVC, and 20% MVC.

3.2 ANN Performance Results

After the training for each ANN model was complete, it was necessary to check if the training was successful and that the model could properly fit the data. Several techniques were used to evaluate the training performance of each ANN model. First, during training and validation the mean squared error (mse) must show a decreasing trend after each iteration of the network and must eventually converge to the best performance. If the mse significantly increased for any of the datasets, it is possible that the data was overfit to that network. The network performance all ten subjects showed similar decreasing mse for each iteration and the best ANN performances were all derived with less than 15 iterations. This technique verified that each network quickly converged to a solution with a small mse and that the training data for each ANN model was not overfit.

The next technique used regression plots to show how well the training, validation, and testing data could predict the output impedance of the network based on the corresponding target impedance. The regression values for all ten subjects can be found in Fig. 7. It is important to compare the regressions for all three testing subsets because any significant differences between them would indicate that the network overfit or extrapolated the data [45]. The regressions for all the training, validation, and testing datasets resulted in R values between 0.98 and 0.997 percent, demonstrating that each model could predict the correct impedance values using data that was not used to train the network. The regression plots verified that the models did not overfit the data and that each model only displayed small deviations between the target and output impedance.

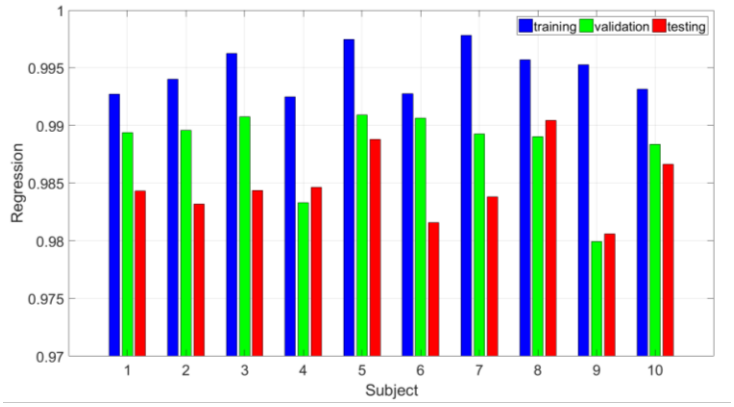

Figure 7. Training, Validation, and Testing regression performance for the ANN models of all subjects.

3.3 ANN Impedance Estimation

The resulting average ANN impedance estimation from the ANN model for the representative subject can be found as the solid line in Fig. 8. These results are compared with the results from the impedance estimation used as the target to the ANN, shown by the dashed line. The maximum relative errors between the target and output impedance magnitude curves in Fig. 8 were 10.2% error for relaxed muscles, 4.5% error for 10% MVC, and 2.5% error for 20% MVC results. To reduce the amount of error even further, additional testing could be performed to create a larger dataset for each subject. This would increase the amount of training data, and create a model that could generalize better to new data. In addition, an interesting observation is that the ANN output impedances follow a smoother curve than the experimentally determined target impedance. This could make this method a useful option for impedance modulation in prosthetic control.

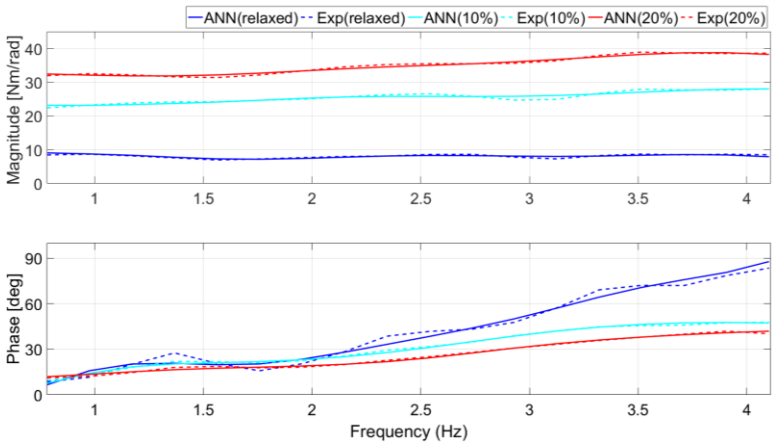

Figure 8. Results of the averaged ankle impedance estimated from the ANN model and the system identification approach for a representative subject with relaxed muscles, 10% MVC, and 20% MVC.

The ANN output impedance estimations for the other nine subjects showed comparable results to the representative subject. Fig. 9 shows the distribution of relative errors between the average target and output impedance magnitude curves across five trials for the relaxed, 10% MVC, and 20% MVC tests. This technique is useful to determine if there are any outliers caused by the network estimation. Each histogram has a bin interval size of five percent error, and the bin height was normalized to the probability of selecting an error within the bin interval. The relative errors for the magnitude of the 10% MVC and 20% MVC trials were within 10% error for all subjects. In addition, the relative error for the relaxed muscle trials were within 15%, except for Subject 1. This subject had four frequency points that were greater than 15% error because the averaged impedance curves had a magnitude of less than 1 Nm/rad. When the relative error was computed, slight differences in impedance exaggerated the percentage of error. The average absolute error for this subject was ±0.44 Nm/rad.

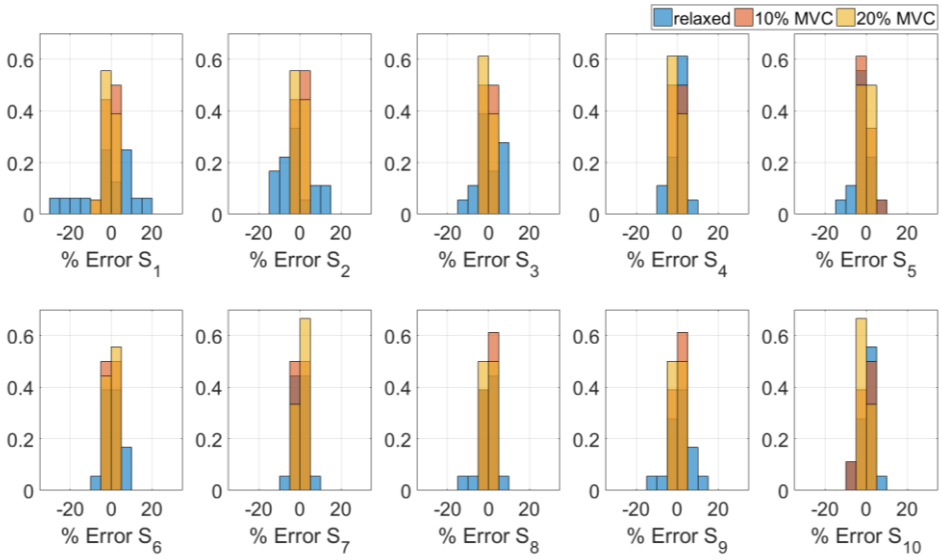

Figure 9. Relative error histogram between the ANN target and output impedance magnitudes for ten subjects with relaxed muscles, 10% MVC, and 20% MVC.

The overall goal of this study was to determine if a neural network could model the relationship between human ankle impedance and lower extremity muscle activations. Based on the results of this study, the trained neural networks for each subject could accurately estimate the ankle impedance in the transverse plane without requiring information about the ankle torque or angles. This is not a trivial task, as the relationship between muscle activation and ankle impedance in nonlinear. The results of this study provide preliminary design parameters for impedance modulation control of an ankle-foot prosthesis.

4 Future Work

This study modeled the relationship between ankle impedance and muscle activity using an ANN for each individual subject. Modeling a neural network to encompass input muscle signals from multiple subjects was challenging because of the variation in both ankle impedance and EMG signals among subjects. Future work could create a more versatile ANN model that can use input muscle data from multiple subjects and accurately predicting ankle impedance without having to retrain the ANN. One method could be to use the biometric data of the subject to determine the appropriate impedance ranges and use their normalized EMG signals to determine the corresponding impedance magnitude. For example, a male subject who is between the ages of 26-28 and has a height between the ranges of 180- 190 cm would have a specific range of impedance magnitudes. A larger database is required to continue the work of this hypothesis.

In addition, future work will look to determine the relationship between the lower extremity muscle activation through measuring their surface electromyography (EMG) signals and time-varying impedance of the ankle during walking maneuvers. A series of gait studies will determine the time-varying impedance of the ankle and corresponding muscle activation levels during different walking maneuvers, such as straight walking and turning. Together, the ankle impedance and EMG measurements will be used to train and validate an ANN model. This relationship will improve our understanding of the role of ankle during an agile gait and can also be incorporated into the control system for powered ankle-foot prostheses.

To accomplish this proposed work, a few challenges need to be addressed regarding the surface EMG measurements and the impedance estimation algorithm. First, while the use of EMG sensors to measure muscle activity can be useful, there can often be variations in the signal measurements. Typically, these are caused by muscle fatigue, sweat on the surface of the skin, or sensor placement on the muscle. These uncertainties must be accounted for while measuring muscle activation levels during walking. In addition, new methods for processing the EMG measurement must be determined as the activation levels will no longer remain constant throughout the experiment.

Similarly, the stochastic system identification method used to determine the impedance of the ankle assumes time-invariant ankle impedance. For this experiment, the subject held their muscle contractions constant for at least 60 seconds to be able to approximate the impedance transfer function in the frequency domain. However, during walking the impedance of the ankle is constantly changing to provide both shock absorption and propulsion to the body. Stochastic identification would not be a plausible method to estimate the impedance. Other methods based on parameter estimation and function optimization must be utilized to estimate the time-varying impedance of the ankle.

5 Conclusion

The lives of many trans-tibial amputees can be improved by developing new methods for controlling ankle-foot prostheses that allow for more natural gait. To accomplish this, understanding the function of a healthy human ankle is necessary. This report presents the results of a novel approach to estimate the nonlinear relationship between lower extremity muscle signals and the mechanical impedance of the ankle in the transverse (EI) plane.

During the experiments, pseudo-random perturbations were applied to the ankle and the resulting torques and angles were recorded at three different levels of muscle activation. A stochastic system identification method used the torque and angle data to estimate the ankle impedance in the EI direction for ten unimpaired subjects. The rms of the muscle signals was used as the input matrix to the ANN and the resulting impedance estimation was used as the target matrix. After training, the output impedance estimation based on the EMG signals was within 15% relative error for nine out of ten subjects, and was within ±5 Nm/rad for all subjects.

These results show a promising direction for using neural networks to determine ankle impedance, especially in the control design of a powered ankle-foot prosthesis. Future work will look to further the methods used in this experiment to understand ankle modulation during walking.

6 Reference List

1. Ziegler-Graham, K., et al., *Estimating the prevalence of limb loss in the United States: 2005 to 2050.* Arch Phys Med Rehabil., 2008. **89**(3): p. 422-429.

2. Smith, D.G., Fergason, J.R., *Transtibial amputations*, in *Clinical Orthopaedics and Related Research*. 1999. p. 108-115.

3. Parker, K., E. Hanada, and J. Adderson, *Gait variability and regularity of people with transtibial amputations.* Gait Posture, 2013. **37**(2): p. 269-73.

4. Segal, A.D., et al., *Comparison of transtibial amputee and non-amputee biomechanics during a common turning task.* Gait Posture, 2011. **33**(1): p. 41-7.

5. Rastgaar, M., et al., *Multi-Directional Dynamic Mechanical Impedance of the Human Ankle: a Key to Anthropomorphism in Lower Extremity Assistive Robots*, in *Neuro-Robotics: From Brain Machine Interfaces to Rehabilitation Robotics*, P. Artemiadis, Editor. 2014, Springer: New York. p. 85-103.

6. Ficanha, E.M., et al., *Ankle Angles during Step Turn and Straight Walk: Implications for the Design of a Steerable Ankle-Foot Prosthetic Robot* in *ASME Dynamic Systems and Control Conference (DSCC)*. 2013: Stanford University, Palo Alto, CA.

7. Glaister, B.C., et al., *Mechanical behavior of the human ankle in the transverse plane while turning.* IEEE Trans Neural Syst Rehabil Eng., 2007. **15**(4): p. 552-559.

8. Glaister, B.C., et al., *Video task analysis of turning during activities of daily living.* Gait & Posture, 2007. **25**(2): p. 289-294.

9. Kearney, R. and I. Hunter, *Dynamics of human ankle stiffness: variation with displacement amplitude.* Journal of biomechanics, 1982. **15**(10): p. 753-756.

10. Hunter, I. and R. Kearney, *Dynamics of human ankle stiffness: variation with mean ankle torque.* Journal of biomechanics, 1982. **15**(10): p. 747-752.

11. Weiss, P.L., R.E. Kearney, and I.W. Hunter, *Position dependence of ankle joint dynamics—I. Passive mechanics.* Journal of Biomechanics, 1986. **19**(9): p. 727-735.

12. Weiss, P.L., R.E. Kearney, and I.W. Hunter, *Position dependence of ankle joint dynamics—II. Active mechanics.* Journal of Biomechanics, 1986. **19**(9): p. 737-751.

13. Zinder, S.M., et al., *Validity and reliability of a new in vivo ankle stiffness measurement device.* J Biomech, 2007. **40**(2): p. 463-7.

14. Rastgaar, M.A., et al., *Stochastic estimation of the multi-variable mechanical impedance of the human ankle with active muscles*, in *ASME 2010 Dynamic Systems and Control Conference*. 2010, American Society of Mechanical Engineers. p. 429-431.

15. Lee, H., et al., *Multivariable static ankle mechanical impedance with relaxed muscles.* Journal of biomechanics, 2011. **44**(10): p. 1901-1908.

16. Lee, H. and N. Hogan, *Modeling Dynamic Ankle Mechanical Impedance in Relaxed Muscle*, in *ASME Dynamic Systems and Control Conference*. 2011: Arlington, VA.

17. Ficanha, E.M. and M. Rastgaar, *Stochastic Estimation of Human Ankle Mechanical Impedance in Lateral/Medial Rotation*, in *ASME Dynamic Systems and Control Conference (DSCC)*. 2014: San Antonio, TX.

18. Ficanha, E.M., G.A. Ribeiro, and M. Rastgaar, *Mechanical Impedance of the Non-loaded Lower Leg with Relaxed Muscles in the Transverse Plane.* Front Bioeng Biotechnol, 2015. **3**: p. 198.

19. Lee, H., et al., *Multivariable static ankle mechanical impedance with active muscles.* Neural Systems and Rehabilitation Engineering, IEEE Transactions on, 2014. **22**(1): p. 44-52.

20. Lee, H., H.I. Krebs, and N. Hogan, *Multivariable dynamic ankle mechanical impedance with relaxed muscles.* Neural Systems and Rehabilitation Engineering, IEEE Transactions on, 2014. **22**(6): p. 1104-1114.

21. Lee, H., H.I. Krebs, and N. Hogan, *Multivariable dynamic ankle mechanical impedance with active muscles.* IEEE Trans Neural Syst Rehabil Eng, 2014. **22**(5): p. 971-81.

22. Lee, H., H.I. Krebs, and N. Hogan. *A novel characterization method to study multivariable joint mechanical impedance*. in *Biomedical Robotics and Biomechatronics (BioRob), 2012 4th IEEE RAS & EMBS International Conference on*. 2012. IEEE.

23. Lee, H. and N. Hogan, *Time-Varying Ankle Mechanical Impedance During Human Locomotion.* IEEE Trans Neural Syst Rehabil Eng, 2015. **23**(5): p. 755-64.

24. Ficanha, E.M., G.A. Ribeiro, and M. Rastgaar, *Design And Evaluation Of A 2-Dof Instrumented Platform For Estimation Of The Ankle Mechanical Impedance In*

The Sagittal And Frontal Planes. IEEE/ASME Transactions on Mechatronics, 2016. **21**(5): p. 2531-2542.

25. Ficanha, E.M., et al., *Time-Varying Impedance of the Human Ankle in the Sagittal and Frontal Planes during Straight Walk and Turning Steps*, in *International Conference on Rehabilitation Robotics*. 2017: London.

26. Rouse, E., et al., *Development of a Mechatronic Platform and Validation of Methods for Estimating Ankle Stiffness during the Stance Phase of Walking.* Journal of biomechanical engineering, 2013. **135**(8): p. 10091-10098.

27. Ficanha, E.M., M. Rastgaar, and K.R. Kaufman, *Ankle mechanics during sidestep cutting implicates need for 2-degrees of freedom powered ankle-foot prostheses.* J Rehabil Res Dev, 2015. **52**(1): p. 97-112.

28. Ficanha, E.M., et al., *Design and Preliminary Evaluation of a Two DOFs Cable-Driven Ankle-Foot Prosthesis with Active Dorsiflexion-Plantarflexion and Inversion-Eversion.* Front Bioeng Biotechnol, 2016. **4**: p. 36.

29. N.M. Olson, G.K.K., *Design of a Transtibial Prosthesis With Active Transverse Plane Control.* Journal of Medical Devices, 2015.

30. Pew, C. and G.K. Klute, *Design of Lower Limb Prosthesis Transverse Plane Adaptor With Variable Stiffness.* Journal of Medical Devices, 2015. **9**(3): p. 035001.

31. C. Gopura, R.A.R., et al., *Recent Trends in EMG-Based Control Methods for Assistive Robots.* 2013.

32. Kearney, R. and I. Hunter, *System identification of human joint dynamics.* Critical reviews in biomedical engineering, 1990. **18**(1): p. 55.

33. R. Osu, H.G., *Multijoint muscle regulation mechanisms examined by measured human arm stiffness and EMG signals.* Journal of neurophysiology, 1999. **81**: p. 1458-1468.

34. Osu, R., et al., *Short-and long-term changes in joint co-contraction associated with motor learning as revealed from surface EMG.* Journal of neurophysiology, 2002. **88**(2): p. 991-1004.

35. Ferris, D.P., et al., *An improved powered ankle–foot orthosis using proportional myoelectric control.* Gait & Posture, 2006. **23**: p. 425–428.

36. Kinnaird, C.R. and D.P. Ferris, *Medial Gastrocnemius Myoelectric Control of a Robotic Ankle Exoskeleton.* IEEE Transactions on Neural Systemsn and Rehabilitation Engineering, 2009. **17**(1): p. 31-37.

37. Schollhorn, W.I., *Applications of artificial neural nets in clinical biomechanics.* Clin Biomech (Bristol, Avon), 2004. **19**(9): p. 876-98.

38. Wang, L. and T.S. Buchanan, *Prediction of Joint Moments Using a Neural Network Model of Muscle Activations From EMG Signals.* IEEE Transactions on Neural Systems and Rehabilitation Engineering, 2002. **10**(1): p. 30-37.

39. Sepulveda, F., D.M. Wells, and C.L. Vaughan, *A neural network representation of electromyography and joint dynamics in human gait.* Journal of Biomechanics, 1993. **26**(2): p. 101-109.

40. Kim, H.K., et al., *Estimation of multijoint stiffness using electromyogram and artificial neural network.* Systems, Man and Cybernetics, Part A: Systems and Humans, IEEE Transactions on, 2009. **39**(5): p. 972-980.

41. Dallali, H., et al., *Estimating the multivariable human ankle impedance in dorsi-plantarflexion and inversion-eversion directions using EMG signals and artificial neural networks.* International Journal of Intelligent Robotics and Applications, 2017. **1**(1): p. 19-31.

42. Di Giulio, I., et al., *The proprioceptive and agonist roles of gastrocnemius, soleus and tibialis anterior muscles in maintaining human upright posture.* J Physiol, 2009. **587**(Pt 10): p. 2399-416.

43. Wheeless, C.R., *Wheeless' Textbook of Orthopaedics*. 2012, Duke University Medical Center's Division of Orthopaedic Surgery: Data Trace Internet Publishing, LLC.

44. Santilli, V., et al., *Peroneus Longus Muscle Activation Pattern During Gait Cycle in Athletes Affected by Functional Ankle Instability: A Surface Electromyographic Study*. The American Journal of Sports Medicine, 2005. **33**(8): p. 1183-1187.

45. Hagan, M.T., Demuth, H. B., Beale, M. H., and De Jesus, O., *Neural Network Design*. 2014. p. 900-903.

46. Rastgaar, M.A., et al., *Stochastic Estimation of Multi-Variable Human Ankle Mechanical Impedance.* 2009: p. 45-47.

Appendix A. Biometric data of Subjects

Table 1. Biometric data of subject's gender, age, mass, height, and MVC level.

Subject	Gender	Age	Mass (kg)	Height (cm)	MVC (μvolts)
1.	F	32	52	162	320
2.	F	26	47	168	80
3.	M	20	88	183	180
4.	M	28	100	187	250
5.	M	24	89	174	400
6.	F	19	64	163	80
7.	M	33	78	174	160
8.	M	23	83	180	170
9.	F	22	65	163	180
10.	F	25	53	173	200